5. Carbon-nitrogen coupling and algal-bacterial interactions during an experimental bloom: Modeling a ^{13}C tracer experiment.

Modified after:
Karel Van den Meersche, Jack J. Middelburg, Karline Soetaert, Pieter van Rijswijk, Henricus T.S. Boschker, Carlo H.R. Heip

Limnology & Oceanography 49(3), 862-878

Acknowledgements

We thank Joop Nieuwenhuize for analytical and logistic support, our Eurotroph colleagues for a stimulating research environment and two anonymous reviewers for constructive feedback. The modeling part of this research was performed in the frame of a master's thesis at Ghent University (first author). It has been supported by the European Union (Eurotroph, EVK3-CT-2000-00040) and a PIONEER grant of the Netherlands Organization of Scientific Research (833.02.2002). We thank Wim Vyverman and Luc De Meester for constructive remarks. This is contribution 3260 from the Netherlands Institute of Ecology.

Abstract

We tracked flows of carbon and nitrogen during an experimental phytoplankton bloom of a natural estuarine assemblage from Randers Fjord, Denmark. We used ^{13}C-labeled dissolved inorganic carbon to trace the transfer of carbon from phytoplankton to bacteria. Ecosystem development was followed over a period of 9 days through changes in the stocks of inorganic nutrients, pigments, particulate organic carbon and nitrogen, dissolved organic carbon (DOC), and algal and bacterial PLFA (polar-lipid derived fatty acids). We quantified incorporation of ^{13}C in phytoplankton and bacterial biomass by carbon isotope analysis of specific PLFA. A dynamic model based on unbalanced algal growth and balanced growth of bacteria and zooplankton adequately reproduced the observations and provided an integral view of carbon and nitrogen dynamics. There were three phases with distinct carbon and nitrogen dynamics. During the first period nutrients were replete, an algal bloom was observed, and carbon and nitrogen uptake occurred in a constant ratio. Because there was little algal exudation of DOC, transfer of ^{13}C from phytoplankton to bacteria was delayed by one day compared to labeling of phytoplankton. In the second phase, exhaustion of dissolved inorganic nitrogen resulted in decoupling of carbon and nitrogen flows due to unbalanced algal growth and the exudation of carbon-rich dissolved organic matter by phytoplankton. During the final, nutrient-depleted phase, carbon and nitrogen cycling were dominated by the microbial loop and there was accumulation of DOC. The main source (60 %) of DOC was exudation by phytoplankton growing under nitrogen limitation. Heterotrophic processes were the main source of dissolved organic nitrogen (94%). Most of the carbon exudated by algae was respired by the bacteria and did not pass to higher trophic levels. The dynamic model successfully reproduced the evolution of trophic pathways during the transition from nutrient replete to depleted conditions, indicating that simple models provide a powerful tool to study the response of pelagic ecosystems to external forcings.

5.1 Introduction

Understanding the transfer of carbon and nutrients between the environment, autotrophs and heterotrophs is key to further our knowledge on biogeochemical cycling and ecosystem functioning and how both relate. Ecologists have long distinguished two trophic pathways in the pelagic environment, i.e. the herbivorous or classical food web and the microbial loop, but now acknowledge the existence of a continuum of trophic structures with the herbivorous food web and the microbial loop as end-members (Legendre & Rassoulzadegan, 1995). The different trophic pathways within this continuum may shift seasonally or following a disturbance

with the result that nutrient use changes at the community level. Similarly, the traditional biogeochemical paradigm that the use and release of nutrients at the ecosystem level obeys a simple constant stoichiometry (Redfield ratio), recorded in the fixed ratio of C to N and P in seston (Redfield *et al.* , 1963), has been successfully challenged. Temporal decoupling of carbon and nutrient dynamics has been reported repeatedly following bloom events (Engel *et al.* , 2002; Wetz & Wheeler, 2003) and is reflected for instance in temporal accumulation of carbon-rich dissolved organic matter (Duursma, 1961; Sondergaard *et al.* , 2000), increases in particulate C:N ratio and formation of transparent carbon-rich exopolymeric particles (Alldredge *et al.* , 1995). Decoupling of carbon and nutrient cycling at the community level is related to the different abilities of autotrophs and heterotrophs to maintain homeostasis (Sterner & Elser, 2003) and to the different dynamics of the particulate and dissolved organic matter pools (Banse, 1994).

In all organisms, the carbon and nitrogen cycles are closely linked (Sterner & Elser, 2003), but the coupling between carbon and nitrogen economy in heterotrophs (bacteria, higher trophic levels) and algae differs in many respects. First, bacteria have a higher basic nitrogen requirement for proteins, nucleic acids etc. and therefore a lower C:N ratio than most algae. Heterotrophs also maintain relatively narrow stoichiometric ranges for C and N in their biomass. This contrasts to resource investments in algae that are not as closely coupled but regulated by their physiological condition. To secure growth, their carbon and nitrogen acquisition must be coordinated, but not necessarily coupled in time and the C:N ratio of algae can be quite variable. Algae use the carbon acquired by photosynthesis during the day for nitrogen assimilation and biosynthesis during the night till exhaustion of photosynthesis products. In contrast to phytoplankton, heterotrophs are not directly dependent on light intensity, but they need the products produced by the algae for growth. Higher trophic levels derive their energy from algal tissue either directly (grazers) or indirectly (predators). The direct link from algae to bacteria is via dissolved organic matter, the main source of bacterial carbon and the preferred source of bacterial nitrogen (Kirchman, 1994; Wheeler & Kirchman, 1986). Algae produce dissolved organic matter (DOM) through lysis, passive leakage or by exudation of carbon-rich material (Anderson & Williams, 1998), but there are other sources of DOM as well, either indirectly linked or independent from algal dynamics. These include enzymatic hydrolysis of particulate material through bacteria (Smith *et al.* , 1992), sloppy feeding and incomplete digestion by grazers (Jumars *et al.* , 1989) and bacterial mortality after viral lysis (Cotner & Biddanda, 2002). Conversely, algae depend on the ammonium regenerated by bacteria and higher trophic levels for their growth. All this indicates that the carbon and nitrogen metabolism of algae and heterotrophs are related, but not necessarily synchronized. For instance, there is ample evidence that bacteria re-

spond to increased primary production with a variable time lag of a couple of days (Ducklow *et al.* , 1993).

Our ability to test or quantify the couplings of algae and heterotrophs in nature or between nitrogen and carbon cycles depends on acquiring a good data set. Such data should be of sufficient temporal resolution and include the necessary measurements that can constrain the many unknown fluxes. Simple standing stock measurements may give indication of how the system works, but are generally not sufficient to make quantitative statements with reasonable accuracy (Vallino, 2000). This is because biomass changes are the net result of many processes that operate at the same time. The deliberate introduction of a tracer such as ^{13}C-labelled dissolved inorganic carbon (DIC) under controlled conditions, and its consequent tracking into the various components, provide valuable extra constraints (Cole *et al.* , 2002; Lyche *et al.* , 1996; Norrman *et al.* , 1995). It allows pinpointing which pathways are significant and to identify the main players of the ecosystem. Through analysis of the concentration of specific biomarkers for algae and bacteria and the appearance of label in these substances (Boschker & Middelburg, 2002), it is now possible to resolve algal-bacterial interactions using stable isotopes (Middelburg *et al.* , 2000).

In combination with mathematical modeling, such data may also serve to estimate the fluxes and turnover rates. To date a number of physiologically-based models exist that describe the uncoupling of C and N assimilation in algae (so-called unbalanced growth models), either through the build-up and consumption of energy storage reserves (Lancelot & Billen, 1985) or of an intracellular nitrogen pool (Droop, 1973; Tett, 1998). These formulations have proven their worth in simulations of culture data (Geider *et al.* , 1998) and seasonal data (Flynn & Fasham, 2003; Lancelot *et al.* , 1991; Soetaert *et al.* , 2001). Similarly, a suite of models exists that explicitly deal with C and N acquisition in bacteria (Anderson & Williams, 1998). While these formulations provide an idealized outline how algal and bacterial organisms function, we still need to progress in our understanding and prediction capacity of how both work together in an ecosystem context.

In this paper we used a combined experimental-modeling approach to investigate C and N dynamics within the microbial domain during an exponential bloom. We specifically tried to assess the coupling between algae and bacteria and between carbon and nitrogen during and after the bloom. To do so, we added ^{13}C-labelled DIC and followed the fate of ^{13}C for 9 days within an enclosure. The biomass and incorporation of label into bacteria and algae was tracked through specific polar lipid derived fatty acids (PLFA). A coupled carbon-nitrogen-^{13}C model was then used to quantify the carbon and nitrogen fluxes between the different compartment and organisms during the transition from nutrient replete to depleted conditions.

5.2 Materials and Methods

5.2.1 Experiment

The experiment took place in Randers Fjord Estuary, Denmark (56°35'N, 10°22'E) from 21 - 30 August 2001. Water was collected from the freshwater end of the Randers Fjord. Salinity of the water was 0.2 and riverine dissolved inorganic nutrient and carbon concentrations were high (58 mmol N m^{-3}, 1.1 mmol P m^{-3}, 226 mmol Si m^{-3} and 2.1 mol C m^{-3}), though comparable to those in coastal upwelling systems except for the high dissolved inorganic N:P ratio and Si concentrations. At noon, 21 August 2001, two 80 liter, transparent carboys were filled with 60 liter ambient water and 10 ml 0.5 mol L-1 ^{13}C-DIC (>98 % ^{13}C) was added to a final concentration of 8.3 μmol L-1 (< 3 % of total stock). After closing the containers, they were left floating in the water. For a period of 9 days, the water was sampled 8 times (after 0, 4, 24, 48, 72, 120, 168, 204 hours) and the temperature and pH were measured. The carboys were vigorously mixed manually before sampling about 4-6 liters. About 750 ml of water was filtered through pre-weighted, pre-combusted Whatman GF/F filters, which were stored at -20°C and later analyzed for particulate nitrogen (PN) and organic carbon (POC), using an elemental analyzer (Nieuwenhuize *et al.* , 1994). The carbon isotopic composition of the particulate material was measured using a Carlo Erba Elemental analyzer coupled on line to a Finnigan Delta S isotope ratio mass spectrometer. GF/F filtered water was stored frozen or at 4 °C and later analyzed for various compounds. Concentrations of silicate, phosphate, ammonium, nitrate, and nitrite were measured by automated colorimetric techniques (Middelburg & Nieuwenhuize, 2000a). For analysis of photosynthetic pigments, another portion of water (500 to 750 ml) was filtered through GF/F filters which were stored frozen until analysis by HPLC (Barranguet *et al.* , 1997). Samples for DIC and δ^{13}C-DIC were collected in headspace vials (50 ml) and preserved with mercury chloride. In the laboratory, a He headspace was created and the concentration and isotopic composition of carbon dioxide in the headspace was measured using an Elemental Analyzer coupled to a Finnigan Delta XL isotope ratio mass spectrometer (Moodley *et al.* , 2000). Samples for DOC (20 ml) were filtered through pre-combusted GF/F filters, stored frozen and analyzed using a combined UV-wet oxidation technique. About 2 liters of water was filtered through GF/F filters for subsequent measurement of PLFA concentration and isotopic composition. Briefly, algal and bacterial PLFA were extracted according to Boschker *et al.* (1999) and Middelburg *et al.* (2000) and measured using GC-FID (gas chromatography with Flame Ionization Detection). Incorporation of ^{13}C in phytoplankton and bacterial biomass was quantified by carbon isotope analysis of specific PLFA, using gas chromatography-combustion isotope ratio mass spectrometry (GC-C-IRMS) (Boschker & Middelburg, 2002). Phytoplankton and

bacterial carbon concentrations were calculated from the PLFA concentrations as described in Middelburg et al. (2000). From the specific bacterial PLFA, total bacterial C concentration can be calculated as

$$C_{bact} = \frac{\sum PLFA_{bact}}{a} = \frac{\sum PLFA_{bact,spec}}{a * b}$$

where a is the average PLFA concentration in bacteria (0.073 g of carbon PLFA per gram of carbon biomass for aerobic environments (Brinch-Iversen & King, 1990), and b = 0.14 g specific bacterial PLFA (i14:0, i15:0 and a15:0) per g bacterial PLFA content (Moodley *et al.* , 2000). Phytoplankton concentration was calculated from the difference between total PLFA and bacterial PLFA as

$$C_{phyto} = \frac{(\sum PLFA - \sum PLFA_{bact})}{c}$$

The average concentration of PLFA in algae (c = 0.046 g PLFA-carbon per g carbon biomass) was estimated by linear regression between $(POC - C_{bact})$ and $PLFA_{phyto}$, assuming that detritus concentrations were negligible at the start of the experiment. This value is significantly higher than what was reported by Middelburg *et al.* (2000), c = 0.035, but including an initial detritus concentration would only increase the estimated value (see below).

5.2.2 Model

The dataset obtained from the enclosure experiments was analyzed with a mathematical model, in order to test the internal consistency of the various measurements and to quantify the fluxes between the compartments. Because of the limited size of the carboys, a vertical gradient was neglected and a zero-dimensional model implemented. The model is driven by photosynthetically active irradiance, imposed as a forcing function (Fig.1). Hourly data were available from the Danish Institute for Agricultural Sciences from a nearby site. In addition, the temperature and the pH, as measured daily in the experiment vessels, were imposed to the model (Fig.1). The model was implemented on a personal computer, in the model environment FEMME (Soetaert *et al.* , 2002) and the code is available upon request. All model equations, parameters and variables are shown in the appendix of this chapter (section 5.5). Equations are based on the model of Anderson & Williams (1998), (hereafter referred to as A&W) but with spatial components eliminated and including a number of essential modifications related to unbalanced algal growth. The model of A&W describes fluxes in terms of nitrogen between three living (bacterial N, phytoplankton N and zooplankton N), one detrital (N), four dissolved organic matter pools (labile and semi-labile DOC and DON) and

two nutrients (nitrate and ammonium). Total carbon fluxes and ^{13}C carbon fluxes accompanying the nitrogen fluxes were first added to this model. As all biological and chemical processes are temperature dependent, a temperature limitation factor is included in every equation term (eq. 1). The data showed significant variations in the C:N ratio of total particulate organic matter, which could not be reproduced with the original A&W model where all particulate constituents have a constant C:N ratio. Therefore, variable C:N ratio in phytoplankton and detritus[1] had to be considered. The variation of the C:N ratio in phytoplankton is based on the unbalanced growth model of Tett (1998), as implemented in the model of Soetaert *et al.* (2001). In this model the N and C uptake (eq. 4,7), are uncoupled through the luxury uptake of dissolved inorganic nitrogen. Also, the detritus breakdown rates were made dependent on the detritus C:N ratio assuming that nitrogen-depleted fractions are more refractory and nitrogen-rich fractions are more labile (Smith & Tett, 2000; Soetaert *et al.* , 2001) (eq. 38-42). A significant decrease in DIC concentration (down to 780 mol C m^{-3}) justified the need to introduce a carbon limitation factor in the phytoplankton carbon uptake rate (eq. 9). Chlorophyll *a* (*Chl a*) concentrations were modeled as described in (Soetaert *et al.* , 2001), depending on the phytoplankton concentration and the phytoplankton C:N ratio (eq. 53-54).

In A&W, DOC is actively released by phytoplankton to compensate the luxury carbon uptake caused by shifts in environmental factors such as light availability and nutrient depletion (Mague *et al.* , 1980; Williams, 1990). Two formulations are presented in A&W: active DOC release as a constant fraction of the primary production, and thus depending on light, or release depending on the nutrient stressed condition of the algae (related to both light and nutrient availability). We implemented the second option (eq. 10) as the model showed an improved accordance between predicted and observed values using this formulation. Unlike A&W however, carbon uptake is not dependent on nutrient limitation (a function of external nutrient concentration), but on the internal C:N ratio in phytoplankton (eq. 7). Extra carbon overflow is calculated as a fraction of the difference between nutrient-limited (actual C:N ratio) and nutrient-saturated growth rate (minimum C:N ratio). This explains the limitation factor in equation 10:

$$\frac{\theta_P - min\theta_P}{max\theta_P} = (1 - \frac{min\theta_P}{max\theta_P}) - (1 - \frac{\theta_P}{max\theta_P})$$

which is the difference between the physiological limitation factors for minimum and actual C:N ratio respectively.

[1]Looking at concentrations of inorganic P (see figure 5.1), P might have been a limiting nutrient even more than N. However, data on P in the various model compartments was limited, and N limitation proved sufficient to show a good model fit (see results). Therefore, the model only includes N and C.

Zooplankton grazing and mortality are modeled as in A&W (eq. 19, 25), and excretion and respiration terms are added in the nitrogen and carbon uptake equation respectively (eq.16). Constant zooplankton stoichiometry (homeostasis) is regulated through excretion and respiration; if the nitrogen content of the ingested food is too high, excess nitrogen is excreted (eq. 23). If the food contains too little nitrogen, the carbon surplus will be respired (eq. 24). The bacterial and DOC-DON dynamics are kept as in A&W (eq. 26 -35) except for the bacterial mortality rate, which is assumed to be proportional to the bacterial concentration (2^{nd} order mortality), as viral infection causing cell lysis increases with the concentration (Cotner & Biddanda, 2002) (eq. 36). The experiments took place in a very small, enclosed environment and DIC concentrations and the pH varied considerably (Fig. 5.1,5.3). As a result, pCO_2 changed from highly supersaturated at the start to undersaturated at the end of the experiment. CO_2 exchange with the atmosphere was therefore considered, similarly as described in Cole *et al.* (2002) (eq. 52). CO_2 partial pressure is calculated in the model using the pH, temperature (both forcing functions), DIC concentration (a state variable) and thermodynamic solubility of CO_2 at the prevailing temperature and salinity (Millero, 1995). The gas piston velocity was obtained from model fitting and has little physical relevance as the air-sea exchange was taking place in closed containers[2].

The ^{13}C cycle was described, following the same pathways as the total carbon ($^{13}C + ^{12}C$) cycle and using the same process parameters. In short, for each C flux, a corresponding ^{13}C flux was calculated, and made proportional with the ^{13}C content of the source compartment:

$$F_{X,^{13}C} = F_{X,C}\frac{X_{^{13}C}}{X_C}$$

where $F_{X,^{13}C}$ and $F_{X,C}$ represent fluxes of ^{13}C and total C respectively, and $\frac{X_{^{13}C}}{X_C}$ is the fraction of ^{13}C in the flux source compartment.

5.3 Results

5.3.1 Experiment

The two enclosure experiments exhibited similar temporal behavior and will therefore be considered as replicates (Fig. 5.1 to 5.3). The experiment started off with low values of particulate organic matter (both living and non-living) with high

[2]As the containers were opened regularly for inspection and for sampling, exchange with the atmosphere could not be ruled out and was therefore included in the model.

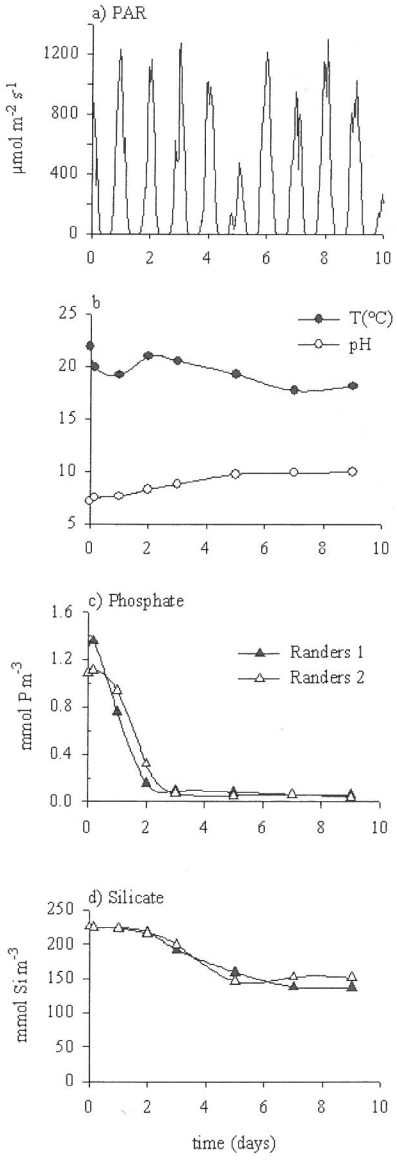

Figure 5.1: Temporal evolution of forcing parameters, dissolved inorganic phosphate and silicate. The two replicate experiments (Randers 1 and 2) are presented with different symbols. a) PAR data measured in air using a LICOR sensor LI-190SA (400-700 nm). Data from Foulum, about 25 km from the center of the city of Randers, Courtesy the Danish Institute of Agricultural Sciences, b) temperature and pH, c) dissolved inorganic phosphate, d) dissolved silicate.

C:N ratio (10 mol C mol N^{-1}) and high dissolved inorganic nutrient concentrations (ammonium 1.9 mmol N m^{-3}, nitrate 56.1 mmol N m^{-3}; phosphate 1.1 mmol P m^{-3}; silicate 226 mmol Si m^{-3}). These conditions triggered the onset of an algal bloom ending at noon at day 4. In this period chlorophyll concentrations increased exponentially almost two orders of magnitude (from 3.6 to 100 mg *Chl a* m^{-3}, Fig. 5.3f). Following exhaustion of inorganic nitrogen and phosphate (Fig. 5.1c, 5.2c,d) the bloom terminated. Ammonium (Fig. 5.2d) was consumed first, followed a few days later by nitrate (Fig. 5.2c). Dissolved Si remained well above limiting concentrations (Fig. 5.1d). The decrease in the C:N ratio observed in the particulate organic matter at this stage (from 10 to 7 mol C mol N^{-1}) reflects the growth of fresh algal biomass (with low C:N ratio) that dilutes the refractory detrital matter present (Fig. 5.2c).

The post-bloom phase is characterized by low nutrient conditions with concentrations of $\simeq$1 mmol NO_3^- m^{-3} and $\simeq$0.2 mmol NH_4^+ m^{-3}. During this phase,

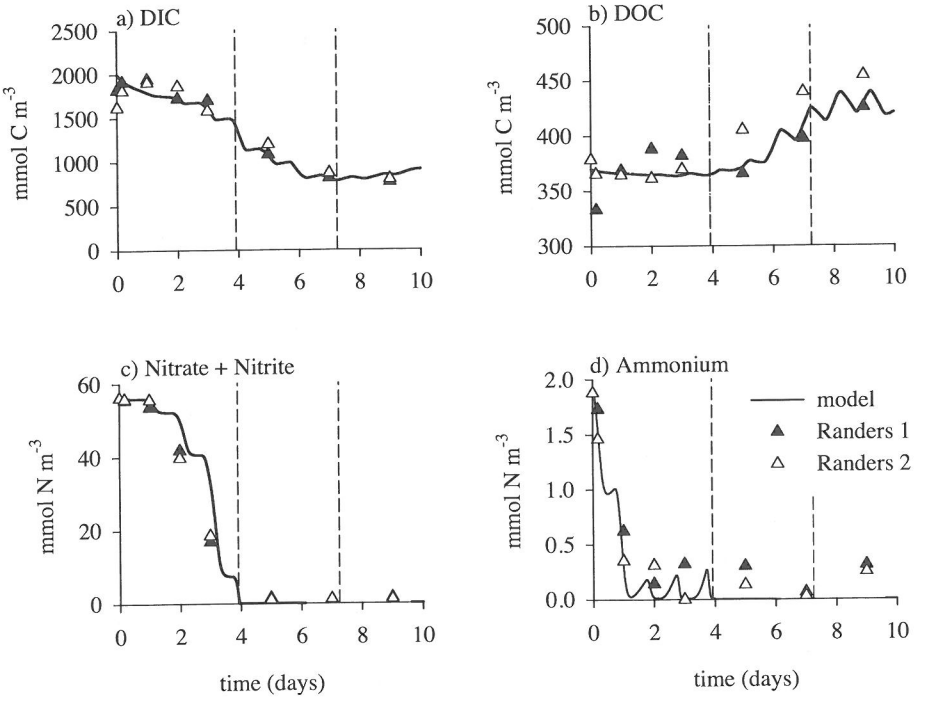

Figure 5.2: Temporal evolution of dissolved pools for the two enclosure experiments (Randers 1 and 2) and model results (solid line). The three phases are denoted by the vertical dashed line.

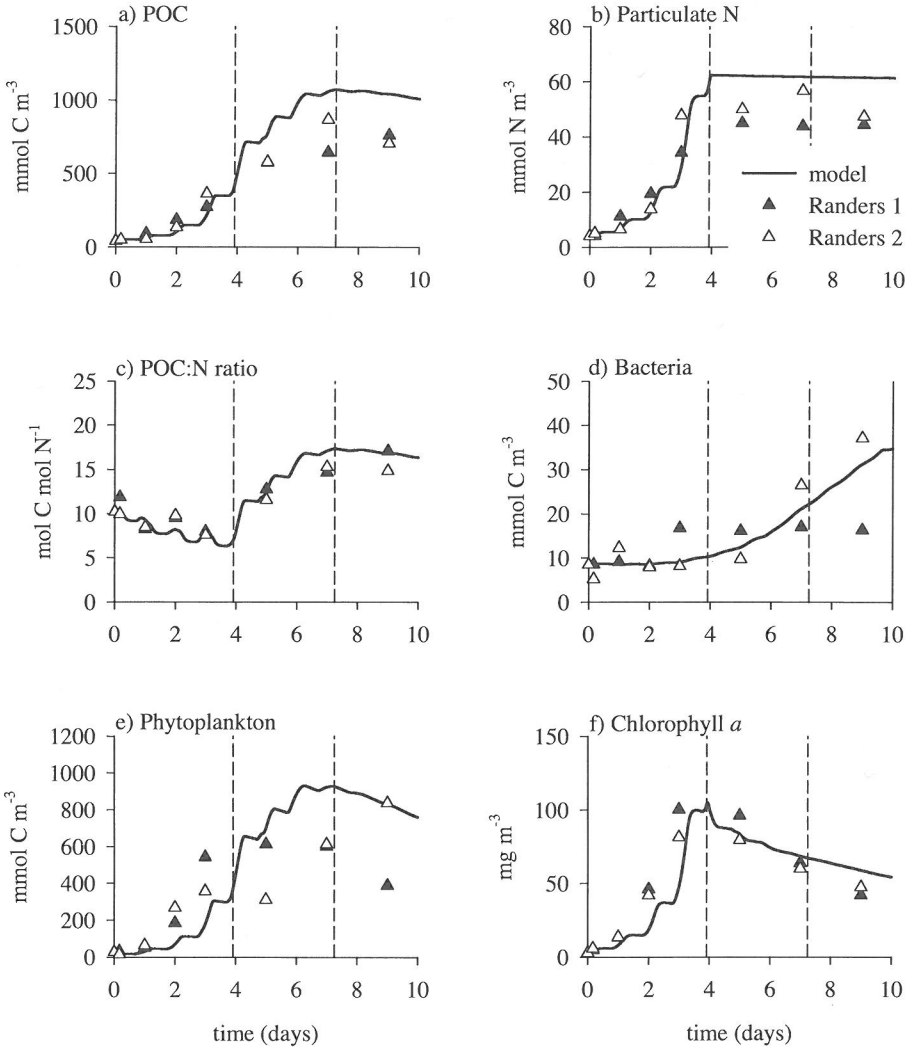

Figure 5.3: Temporal evolution of particulate pools for the two enclosure experiments (Randers 1 and 2) and model results (solid line). The three phases are denoted by the vertical dashed line.

chlorophyll concentrations decreased significantly, from 100 mg m^{-3} at day 4 to 50 mg m^{-3} at day 9. Phytoplankton carbon content based on PLFA concentrations also decreased, but less pronounced (Fig. 5.2e). The nutrient exhaustion also induced large changes in the physiological status of the algae: the C:N ratio of particulate organic matter more than doubled, up to 16 mol C mol N^{-1}, indicating a decoupling of carbon and nitrogen dynamics in phytoplankton. After that the C:N ratio remained more stable. DOC concentrations were quasi-constant at first, but increased from 370 to 440 mmol C m^{-3} after the bloom (Fig. 5.2b). The bacterial biomass, derived from PLFA concentrations (Fig. 5.3d), followed DOC concentrations.

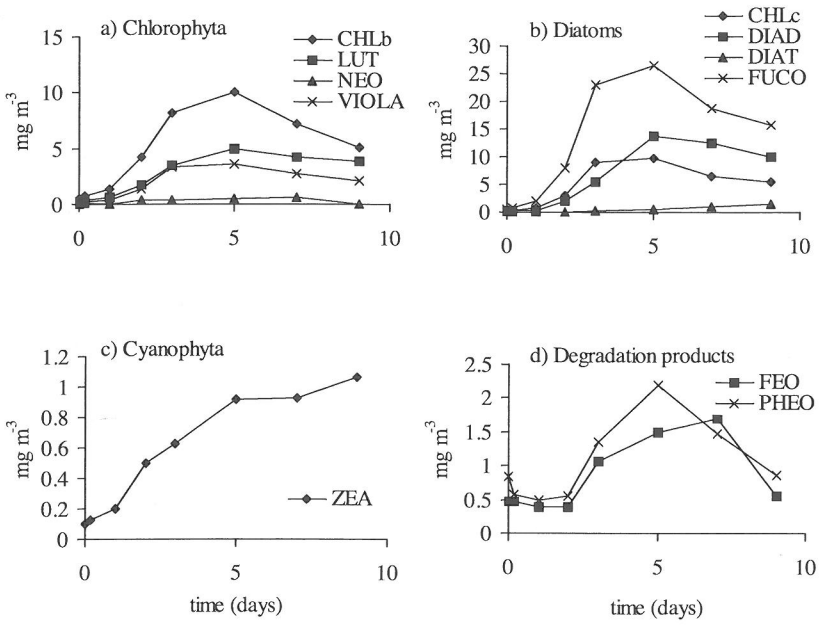

Figure 5.4: Temporal evolution of photosynthetic pigments characteristic for a) green algae, b) diatoms, c) cyanobacteria and d) degradation products. CHLb = Chlorophyll b, LUT = Luteine, NEO = Neoxanthine, VIOLA = Violaxanthine, CHLC = Chlorophyll c, DIAD = Diadinoxanthine, DIAT = Diatoxanthine, FUCO = Fucoxanthine, ZEA = Zeaxanthine, FEO = Pheophytine, PHEO = Pheophorbide.

Pigment analysis indicated that there was a slight dominance by green algal pigments (chlorophyll b, luteine, neoxanthine, violaxanthine) at the start, and an increasing preponderance of diatom pigments (chlorophyll c, diadinoxanthine, diatoxanthine, fucoxanthine) towards the end (Fig. 5.4). The ratio of diatom to chlorophyte pigments changed from 1.1 in the exponential phase to 3.0 after the

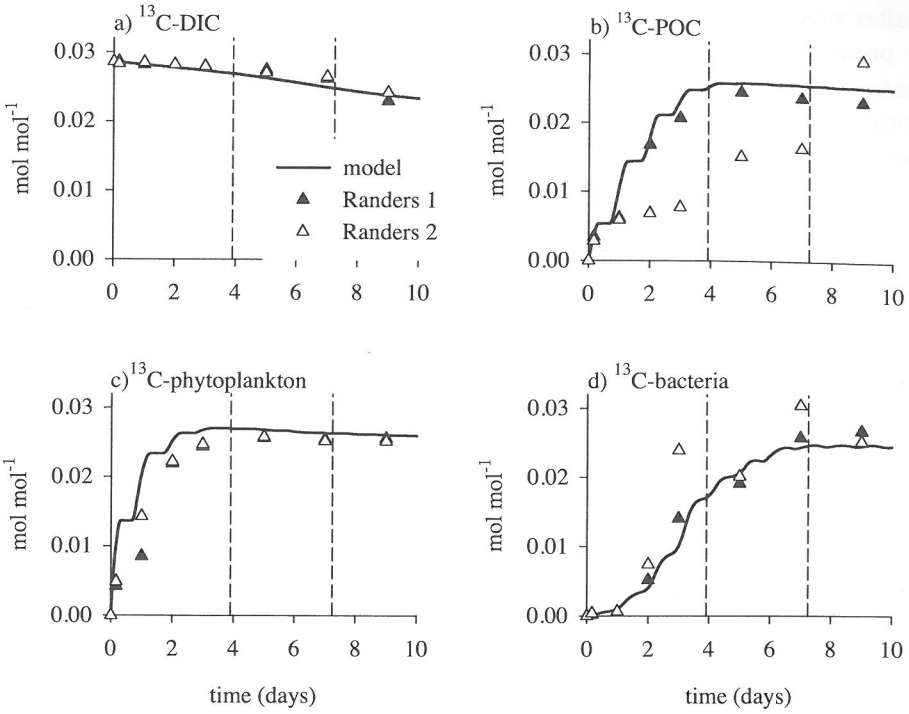

Figure 5.5: Temporal evolution of 13C fractions in DIC, POC and algal and bacterial carbon pools for the two enclosure experiments (Randers 1 and 2) and model results (solid line).

bloom and this dominance of diatoms is consistent with silicate concentrations that remained well above limiting values (Fig. 5.1d). The concentration of cyanobacterial pigments (zeaxanthine) remained low, although they kept increasing until the end of the experiment. Concentrations of algal specific PLFA showed the same trend as algal pigments and support the dominance of diatoms and green algae in the enclosures (data not shown).

Carbon-13 was added as a deliberate tracer to follow carbon transfer from the DIC pool to algae and then to bacteria. After adding ^{13}C-DIC, the δ^{13}C of DIC increased to 2675 ‰, equivalent to a ^{13}C/C fraction of 2.5%. δ^{13}C-DIC decreased to $\simeq$2200 ‰ towards the end of the experiment. Particulate organic δ^{13}C increased from background values of -29 ‰ to $\simeq$2200 ‰ in about four days due to dilution with newly fixed ^{13}C-rich carbon and then stabilized. This ^{13}C enrichment is more dramatic for phytoplankton δ^{13}C values that increased to >2200 ‰ within three days. Bacterial δ^{13}C increased with a delay of about one day and attained $\simeq$2200

‰ after six days. For comparison with the model, ^{13}C fractions ($^{13}C/(^{13}C+^{12}C)$) are presented rather than δ^{13}C, because they are easier to interpret (Fig. 5.5). The bulk POC, phytoplankton and bacterial pools all reached the same asymptotic enrichment level of 2.5 % indicating that these pools were in isotopic equilibrium at day 5. Summarizing, three phases can be distinguished in the experiment (Fig. 5.2, 5.3): (1) an exponential growth or bloom phase (day 1-3) with sufficient nutrients, (2) an unbalanced growth or intermediate phase (day 4-7) with nutrient depletion and ongoing algal production and (3) a post-bloom or stationary phase (day 8-9) with DOC and bacterial biomass accumulation.

5.3.2 Model initialization

Our dynamic model requires specification of 23 initial conditions. Some of them (ammonium, nitrate, DIC) have been measured directly, but many needed to be estimated. At the start of the experiment, a high POC:PON ratio (10.2 mol C mol N^{-1}) was found. This ratio reflects the C:N ratio of algae and detritus, the two dominant pools contributing to the particulate organic matter pool. Since high C:N ratios of algae are not expected in a nutrient-rich environment, we imposed an initial C:N ratio 6 for phytoplankton and consequently derived an initial refractory detritus fraction with high C:N ratio (20 mol C mol N^{-1}). This refractory material could originate from the common reed fields in the surroundings of the sampling location or other upstream sources. Initial algal carbon and nitrogen contents were estimated from measured chlorophyll using equations 53 and 54 (Table 3 of the appendix). No macrozooplankton was observed in the experiments, and microzooplankton predation was not determined. The decrease of chlorophyll during the second half of the experiments (day 5-9), accompanied by small phytoplankton carbon and POC decreases, could only be reproduced assuming a small initial zooplankton concentration, which in the end reduces phytoplankton due to grazing.

In the model, DOM is divided into three pools: refractory, semi-labile and labile DOM, where the first behaves conservatively. The initial DOC concentration was determined, but the relative amounts of these three pools cannot be measured and were obtained by tuning the model. The size of these three pools affects the bacterial uptake rate of carbon and ^{13}C. Fitting demanded that the initial labile DOC was 0.8% of the total DOC pool (making the initial ratio labile DOC:semi-labile DOC around 8:100), which is within the range of values found in literature (0-6% in marine systems (Carlson, 2002b)). Concentration of DON pools were also not measured and assumed to be 10 % of DOC.

5.3.3 Model tuning

Most model parameters (Table 1 of the appendix) were adopted from either A&W or Soetaert *et al.* (2001), but some parameters related to algal carbon and nutrient acquisition, algal DOM exudation and bacterial dynamics required tuning to adequately reproduce the observation. Using the original algal growth model (Soetaert *et al.* , 2001; Tett, 1998), the algae continued to deplete DIC at the end of the experiment, whereas a stabilization of DIC was observed instead (Fig. 5.3). Therefore, we introduced growth limitation through DIC with a half-saturation constant of 250 mmol C m^{-3} (eq. 9, table 3 of the appendix) to prevent carbon acquisition in the absence of DIC. Although phytoplankton carbon assimilation is modeled as DIC uptake, we are aware that CO_2, a small fraction of DIC, is the actual substrate for most algae. This growth reduction could also be related to the high pH values (Fig. 5.1b), which are detrimental to the integrity of the cell wall. Nitrate and ammonium concentrations decrease abruptly in the phytoplankton bloom phase and the steepness of this decline is governed by their respective maximum uptake rates. The required maximum uptake rates were found to be higher than the values used in e.g. A&W or Soetaert et al. Soetaert *et al.* (2001).

Phytoplankton leakage was diminished from 5 % in A&W to 2 % of the primary production (eq. 2-3, table 3 of the appendix) to reproduce the limited incorporation of ^{13}C in bacterial biomarkers during the initial bloom phase. Phytoplankton respiration was set on 10% of the primary production, well within values observed (between 5 and 15 %, e.g. McAllister *et al.* , 1964; Steemann Nielsen & Hansen, 1959). The importance of active DOC exudation under nutrient limited conditions needed reassessing (Parameter $\gamma 3$, eq. 10, table 3 of the appendix), because in our model with unbalanced algal growth, phytoplankton C:N ratio (eq. 10) regulates this DOC exudation, instead of direct nutrient limitation as in A&W. This process highly influences the course of DOM concentrations and C:N ratios, a value of 0.05 was found to give the best model results, in contrast to 0.26 in A&W. The thus calculated extra DOC produced varied from 0 to 65 % of gross primary production. To prevent DOM accumulation, the labile fraction of produced DOM in the model had to be about 0.65. Preceding modeling studies used fractions varying from 0.1 (A&W) up to 0.9 (Levy *et al.* , 1998) to obtain acceptable correspondence (Christian & Anderson, 2002).

Bacterial growth efficiency (BGE) and maximal DOC uptake rate govern bacterial ^{13}C signature and carbon concentration. The maximal DOC uptake rate was kept as in A&W, but the bacterial growth efficiency had to be altered as lower values of BGE gave better fits. According to del Giorgio & Cole (1998), bacterial growth efficiency for Danish estuaries has a minimal value of 0.19 and this value was therefore adopted. Bacterial mortality only affects bacterial concentration, not

the bacterial ^{13}C signature; this process is modeled with a quadratic term (in contrast to A&W) and the bacterial specific mortality term mB was obtained by fitting bacterial biomass accumulation.

5.3.4 Model results

Although most model parameters were taken from the literature it appears that the model captures both the dynamics and size of dissolved and particulate pools (Fig. 5.2, 5.3 and 5.5). The model appears to overpredict POC, PON and algal concentrations towards the end of the run. This can be attributed either to an underestimation of zooplankton grazing, to algal growth on the surfaces or to sinking of particulate matter on the bottom of the carboys. Those attached or deposited particles are included in the model (as they affect the other components), but not in the measurements, which are based on water samples only. The model was forced by hourly irradiance data and therefore generates daily fluctuations in many variables, that either directly (e.g. phytoplankton C) or indirectly (e.g. DOC) depend on primary production. This diurnal variability cannot be discerned in the data because of the daily sampling intervals.

The overall good fit gives us confidence that model-based flux estimates are realistic. Moreover, a posteriori comparison of model output for day 1 of the enclosure experiment compares well with independent rate measurement for oxygen dynamics and nitrogen uptake made for the same station during the same week. Model-based rates of net community production and respiration (22 and 6.9 mmol m^{-3} d^{-1}) are consistent with those found during 24 hour *in situ* incubations (19.8 and 7.3 mmol m^{-3} d^{-1}, respectively, Gattuso, personal communication). The total nitrogen uptake predicted by the model (5.2 mmol m^{-3} d^{-1}) is somewhat higher than the sum of ammonium, nitrate, urea and dissolved free amino acids uptake measured during 2 hour incubations (4.8 mmol m^{-3} d^{-1}; Veuger et al., 2004).

Fluxes between the compartments, averaged over the three phases (bloom, intermediate and stationary), were calculated and shown in Fig. 5.6. The magnitude and fate of phytoplankton production is in Table 5.1 and the characteristics of the microbial loop are in Table 5.2.

In the phytoplankton bloom phase (Fig. 5.6a), phytoplankton production was only light-limited and most of the carbon and nitrogen assimilated resulted in algal biomass accumulation (84 and 93 % for C and N, respectively). Only a small fraction (2%) of the assimilated carbon and nitrogen was released to the dissolved organic pool or lost by predation and senescence mortality (3.4 and 3.9 % for C and N, respectively; Table 5.1). Heterotrophic mechanisms contributed most to the formation of dissolved organic matter (56 and 63% in terms of C and N respectively), which was produced with an average C:N ratio of about 7. The

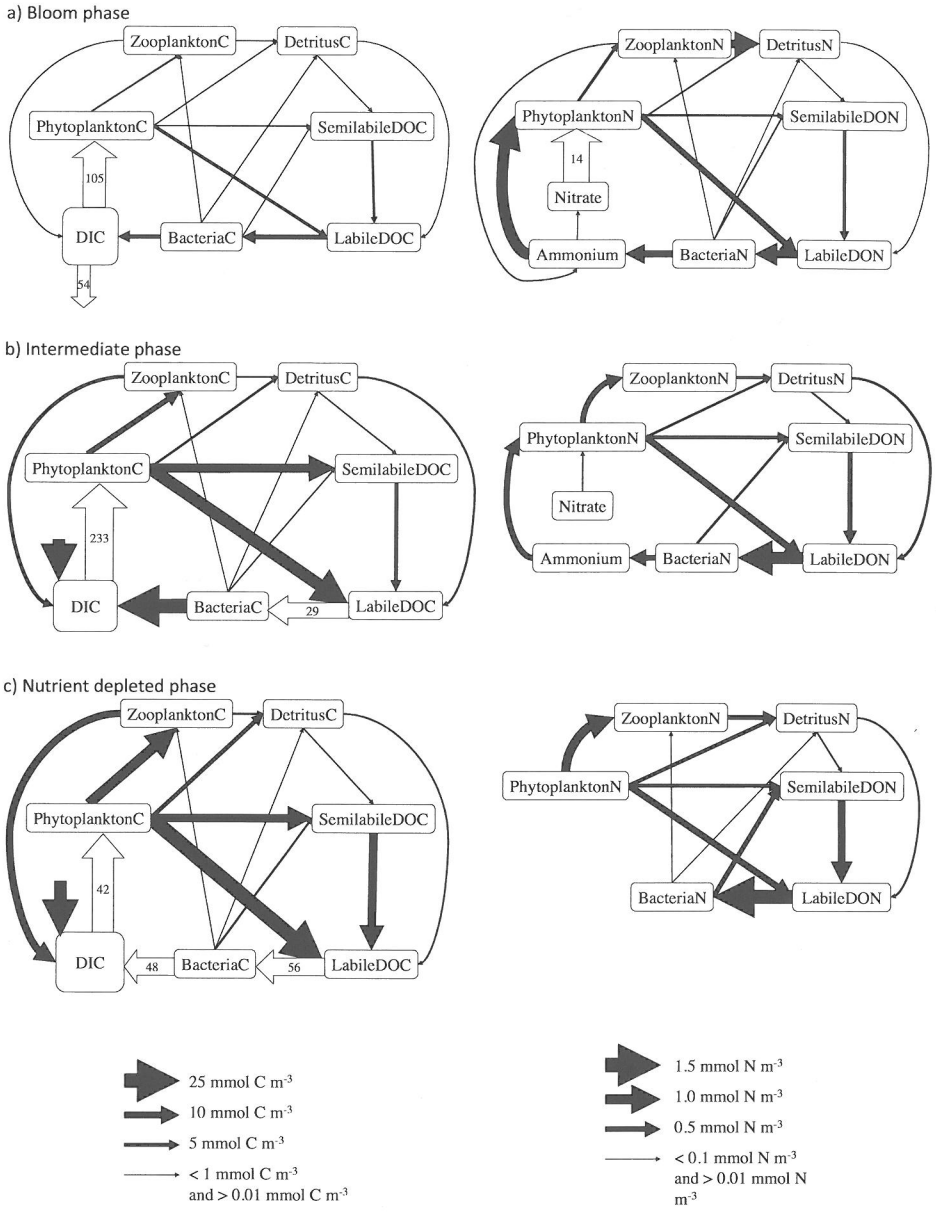

Figure 5.6: Carbon (left) and nitrogen (right) flows during the three phases; the arrow thickness of the black arrows is proportional to the flux rate. Fluxes larger than 25 mmol C m-3 d-1 and 1.5 mmol N m-3 d-1 respectively are represented with open arrows, with the flux indicated in mmol m-3d-1. Fluxes below 0.01 mmol m-3d-1 are not shown. a) bloom phase (day 1-3); b) intermediate, unbalanced growth, phase (day 4-7); c) final, nutrient-depleted phase (day 8-9).

Table 5.1: Magnitude and fate of the phytoplankton primary production (PP) and N uptake. Rates in mmol C m^{-3} d^{-1} and mmol N m^{-3} d^{-1}, concentrations in mmol m^{-3}.

	bloom	intermediate	nutrient limited
Phytoplankton C	114.3	786.7	881.8
Gross PP	118.3	263.7	51.3
>growth	98.8	186.5	-21.4
>respiration	13.0	30.4	9.4
>mortality	4.0	17.7	29.9
>DOC exudation	2.5	28.7	33.3
Phytoplankton N	17.8	52.5	45.0
N uptake	15.3	0.6	0.0
>growth	14.3	-1.0	-2.1
>mortality	0.6	1.6	2.1
>DON exudation	0.3	0.01	0.0

uptake of dissolved organic matter by bacteria was used for growth (19 and 30 % for C and N, respectively), respiration (81% of C) and ammonium regeneration (70 % of N; Table 5.2). In this phase, there is an efflux of CO_2 because of initial high pCO_2 values.

In the intermediate, unbalanced growth phase (Fig. 5.6b), the carbon cycle had a pattern similar to the bloom phase, while the nitrogen cycle showed the characteristics of a nutrient-limited ecosystem. Gross primary production was about twice that during the bloom phase, but biomass specific gross primary production was only 33% of that during the previous period. About 71% of this assimilated carbon added to phytoplankton biomass, some 11% was released as DOC mainly by exudation and about 7% was lost by zooplankton grazing and mortality. In contrast, algal nitrogen uptake dropped to very low values and was not sufficient to overcome losses by mortality, such that algal nitrogen content decreased in this phase. DOC production came from algal exudation (60 %) and heterotrophic mechanisms (40 %), while almost all DON was produced by heterotrophic processes (>99%). Algal exudation was high to overcome excess carbon assimilation and this resulted in an overall DOC:DON production ratio of >29. The DON consumed by bacteria was mainly used for growth (73%), the remaining 27 % was excreted as ammonium.

In the final, stationary phase (Fig. 5.6c), both carbon and nitrogen acquisition of the phytoplankton were limited. Photosynthesis and carbon fixation were limited by the algal physiological condition (as represented by the high internal C:N ratio) while nitrogen uptake was zero because there was no dissolved inorganic nitrogen.

Table 5.2: Characteristics of the bacterial loop. Rates in mmol C m^{-3} d^{-1} and mmol N m^{-3} d^{-1}, concentrations in mmol m^{-3}.

	bloom	intermediate	nutrient limited
Bacterial C	8.9	15.1	26.5
DOC production	5.8	48.0	59.9
By exudation	2.5	28.7	33.3
By heterotrophic mechanisms	3.3	19.3	26.6
DOC uptake	7.2	30.2	59.7
Bacterial growth	1.4	5.7	11.3
Bacterial N	1.8	3.0	5.2
DON production	0.8	1.6	2.3
By exudation	0.3	0.01	0.0
By heterotrophic mechanisms	0.5	1.6	2.3
DON uptake	0.9	1.5	2.2
Bacterial growth	0.3	1.1	2.2

Neither C nor N assimilation was sufficient to maintain a positive balance and 65% of photosynthetic carbon products were exudated. Mortality (zooplankton grazing, senescence) was responsible for the decline of the algal concentration and kept increasing despite the decline in phytoplankton biomass (Fig. 5.2 e, f). Both carbon and nitrogen cycling were dominated by the microbial loop in this phase. Similar to the intermediate phase, DOC was derived from algal exudation (56%) and heterotrophic mechanisms (44 %), while all DON production came from heterotrophic mechanisms, such as mortality, grazing and detritus breakdown. The overall DOC:DON production ratio was 27 due to exudation of carbon-rich DOM by algae. In this post-bloom phase, all DON consumed served growth of the bacteria and there was no ammonium excretion.

5.4 Discussion

Algae and bacteria are exposed to continuously varying environmental conditions. These fluctuations have major consequences for their interaction and for their carbon and nitrogen cycle. We have induced changes in the environment by enclosing riverine nutrient-rich waters under batch conditions. Most of our experimental results are consistent with and confirm previous studies of marine systems. However, by administering of a deliberate tracer (^{13}C) and the use of a state-of-the-art ecosystem model, not only do we obtain a more complete and consistent picture

of ecosystem functioning and carbon and nitrogen cycling, but we are also able to quantify the links between algae and bacteria, between carbon and nitrogen dynamics and to sharpen the modeling tools that represent these processes.

Experimental blooms in enclosures and mesocosms have shown exponential growth of algae with tight co-variation of carbon and nutrients, increases in pH and little DOC accumulation as long as nutrients were replete (Alldredge *et al.* , 1995; Antia *et al.* , 1963; Banse, 1994; Engel *et al.* , 2002; Sondergaard *et al.* , 2000). Maximum *Chl a* concentrations were usually observed near the time of nutrient depletion (Alldredge *et al.* , 1995; Engel *et al.* , 2002; Norrman *et al.* , 1995). After nutrient depletion, carbon and nitrogen dynamics were usually decoupled as reflected in the accumulation of DOC (Banse, 1994; Norrman *et al.* , 1995; Sondergaard *et al.* , 2000), increases in particulate C:N ratios due to excess particulate carbon (?Banse, 1994; Engel *et al.* , 2002) and release of carbon-rich DOM (Biddanda & Benner, 1997; Wetz & Wheeler, 2003). Most of these studies involved addition of nutrients and focused on uncoupling of particulate organic carbon and nitrogen dynamics (Alldredge *et al.* , 1995; Engel *et al.* , 2002). Our enclosure experiment with natural river water confirms these literature observations for experimental, marine systems and is also consistent with field observations regarding the uncoupling of carbon and nitrogen dynamics (Sambrotto *et al.* , 1993), the accumulation of carbon-rich DOM following the spring bloom (Duursma, 1961) and the delayed response of bacteria to increased primary production (Ducklow, 1999; Ducklow *et al.* , 1993).

Norrman *et al.* (1995) studied the production and consumption of DOC during an experimental diatom bloom using ^{13}C-bicarbonate as a deliberate tracer; bacteria were traced using nucleic acids as a biomarker. They observed rapid labeling and isotopic equilibration of the POC pool after 7 days and a delayed appearance of ^{13}C in the DOC and bacterial pools. The DOC and bacterial pools did not reach isotopic equilibrium during the 14-day period of the experiment. Our experimental results confirm but also complement those of Norrman *et al.* (1995). In our experiment, the added ^{13}C-bicarbonate was rapidly fixed by phytoplankton resulting in isotope equilibration of phytoplankton carbon by day 3 (Fig. 5.5c). The POC pool, comprising algae, bacteria and detritus, was consequently also rapidly labeled, but equilibration took one day more (Fig. 5.5b). Although full isotopic equilibration of the bacterial carbon pool was reached by day 6 (Fig. 5.5d), there was a delay of at least one day before significant amounts of ^{13}C appeared in specific bacterial PLFA. Norrman et al. did not observe this delay likely because they only measured bacterial ^{13}C content after 3.5 days. In addition, bacteria did not attain full isotope equilibration in their experiments, which they attributed to a potential artefact with the nucleic acid method, the presence of a population of inactive bacteria and the use of old and new DOC by the bacteria. The biomarkers that we used specifically trace active bacteria, which could explain the difference in

extent of isotopic equilibration although differences in the ecosystem functioning (role of background DOC and grazing on bacteria) cannot be ruled out.

5.4.1 Carbon and nitrogen coupling by phytoplankton

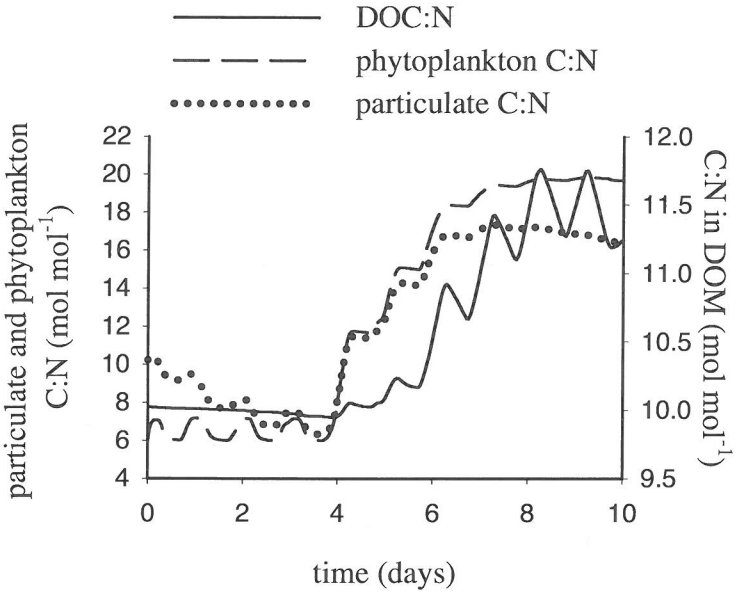

Figure 5.7: Modeled temporal evolution of C:N ratios of the dissolved organic, particulate organic and phytoplankton pools.

In general the ecosystem in our enclosures reacted faster than the other enclosure studies (Alldredge *et al.* , 1995; Engel *et al.* , 2002; Norrman *et al.* , 1995). Consequently, it was possible to clearly delineate three phases with distinct carbon-nitrogen relations rather than the nutrient-replete and nutrient-depleted phase reported in these studies. During the exponential growth phase (day 0-3) the algae are light-limited and take up carbon and nitrogen in constant ratios ($\simeq$ 6) till exhaustion of nutrients. The C:N ratio of the particulate pool decreases from 10 to 7 (Fig. 5.7). During the intermediate, unbalanced growth phase (day 4-7), algal carbon assimilation continues at a high rate while nitrogen assimilation is strongly nutrient limited and the C:N ratio of algae rapidly increases until it is at its maximum level ($\simeq$ 20). This is reflected in the increase of the C:N ratio of the particulate pool from 7 to 16 (Fig. 5.2). Finally, during the stationary phase both algal carbon and nitrogen assimilation are limited, the former by algal physiology,

the latter by the external nutrient concentrations, and the C:N ratio of algal and particulate organic matter pools remain high (day 8-9).

The initial decrease of particulate organic matter C:N ratios and the subsequent increase following dissolved inorganic nitrogen depletion has been reported before (Alldredge *et al.* , 1995; Banse, 1994) and attributed to preferential PON degradation, formation of transparent extracellular particles (TEP) and intracellular increase of algal C:N ratios (Engel *et al.* , 2002). Our model did not include the formation of TEP, but accounted for both preferential particulate nitrogen dissolution and the unbalanced acquisition of carbon and nitrogen in phytoplankton (Fig. 5.7). The initial decrease of C:N ratios (day 0-3) was merely due to dilution of the detrital pool (C:N of 20) with newly formed phytoplankton (C:N$\simeq$ 6), while the increase of C:N ratio after nutrient depletion was consistent with intracellular increases of algal C:N ratios as represented in the unbalanced growth model of Tett (1998).

Unbalanced uptake of carbon and nitrogen allows algae to continue photosynthesis under temporarily nutrient-limited conditions. It is the main cause of the uncoupling of carbon and nitrogen flows in the ecosystem and is expressed by more than doubling of the particulate C:N ratio in 2 days (Fig. 5.7). However, prolonged nutrient limitation results in the exudation of excess carbon as dissolved organic matter. Exudation of carbon-rich DOM by algae is another mechanism by which the flows of carbon and nitrogen are decoupled. It causes increases in DOC:DON ratios with more than 10% in 2 days, lagging about one day behind the rise in particulate C:N ratio (Fig. 5.7).

5.4.2 The production of DOM

Major research efforts during the last decade have revealed a number of mechanisms resulting in the formation of dissolved organic matter (Carlson, 2002a). The relative importance of these different DOM sources is unknown and likely depends on the ecosystem functioning. It is instructive to distinguish between release of DOM by autotrophic and by heterotrophic mechanisms because the governing factors differ. Heterotrophic release of DOM is due to dissolution of particulate detritus (Smith *et al.* , 1992), zooplankton sloppy feeding and incomplete ingestion (Jumars *et al.* , 1989) and lysis of bacteria (Anderson & Williams, 1998). Phytoplankton release may either occur passively (leakage and algal lysis (Bjornsen, 1988), or may consist of active exudation of carbon-rich dissolved organic matter (Biddanda & Benner, 1997; Carlson, 2002a). These two autotrophic DOM sources differ in their C:N ratio and governing factors. While passive leakage is proportional to biomass or production (as we assumed in our model), active exudation depends strongly on algal physiological status, in particular light and nutrient

availability (Obernosterer & Herndl, 1995; Anderson & Williams, 1998; Carlson, 2002a).

The quantitative importance of these processes under *in situ* conditions is still unclear and our study clearly indicates that they may vary rapidly during and following bloom events. During the nutrient-rich bloom period there was no active DOC exudation by phytoplankton and about 2 % of the fixed C and N was released as dissolved organic matter with a C:N ratio similar to that assimilated. Heterotrophic mechanisms accounted for 60 % of total DOM production in that period and the DOM produced had a C:N ratio of 7. During the intermediate and stationary phases algal exudation of recently fixed carbon increased and became the most important DOC source; during the stationary phase 65 % of the carbon assimilated was exudated. Heterotrophic sources of DOM also increased as a consequence of higher concentration of phytoplankton, detritus and bacteria and were relatively N-rich: heterotrophic and autotrophic DOM C:N production ratios were $\simeq$11.7 vs. 28, respectively. Overall, the main source of DOC was phytoplankton exudation (almost 60 % of the DOC production) and not detritus decay. Heterotrophic processes were the main source of DON (94%).

Percentages of extracellular release (PER) of recently fixed carbon vary widely from non-significant up to 70 % of total production (Anderson & Williams, 1998; Carlson, 2002a; Norrman *et al.* , 1995). This variability has been related to many factors including nutrient availability, phytoplankton size and net community production (Teira *et al.* , 2001). It is unclear whether the increase in DOC release under nutrient-stressed conditions is due to the preponderance of small cells with higher surface/volume ratios and therefore higher capacity of passive leakage of DOC (Bjornsen, 1988) or whether it relates to the physiological condition of the algae (Dubinsky & Berman-Frank, 2001) or a combination of both. By implementing the stress-dependent formulation for DOC exudation as prescribed in A&W, we chose for the latter explanation. First of all, because of the large changes in the particulate C:N ratio, which demonstrated unbalanced growth of phytoplankton and thus changing physiological conditions that preceded the increases in DOC concentrations. Secondly, there is no indication that a shift towards smaller cells occurred in the experiments; on the contrary, inspection of the pigment concentrations reflect a relative increase in diatoms, which are generally larger than flagellates and green algae. Teira *et al.* (2001) reported high PER values in the oligotrophic Atlantic Ocean with net negative community production and low PER values for upwelling conditions with net community productions. Our enclosure study supports these field observations and also shows that the transition between different levels of phytoplankton DOC exudation can be rapid.

5.4.3 Algal-bacterial interactions

Heterotrophic bacteria are the major sink for marine dissolved organic matter, which provides the carbon and the majority of the nitrogen for the bacteria. Most of the DOM originates directly (via exudation) or indirectly (via food-web interactions) from phytoplankton and as such bacteria depend on algae for growth. The pool of dissolved organic matter does not always provide enough nitrogen to sustain bacterial growth in which case they will assimilate dissolved inorganic nitrogen (Joint *et al.* , 2002; Kirchman, 1994; Middelburg & Nieuwenhuize, 2000a; Wheeler & Kirchman, 1986) rather than excrete it. Unfavorable DOC:DON ratios for bacterial growth result in particular from algal exudation of carbon-rich dissolved organic matter, a process that is stimulated under nutrient-stressed conditions. Thus, paradoxically, nutrient-stress induces the algae towards production of carbon substrates suitable for growth of bacteria, which then compete with the algae for nutrients (Bratbak & Thingstad, 1985).

Algal-bacterial interactions in our experimental bloom study changed from commensalism at the start to nutrient competition during the final phase. The three phases comprise almost the entire spectrum of trophic pathways (Legendre & Rassoulzadegan, 1995). During the first phase (the herbivory/multivorous food web sensu Legendre & Rassoulzadegan (1995)), bacteria consumed dissolved organic matter from autotrophic and heterotrophic sources and were regenerating ammonium, available for algal growth. The ^{13}C data indicated that there was a delay in the transfer of recently fixed carbon to the bacterial pool (Fig. 5.5). Such a delay between carbon fixation and bacterial response is consistent with many field observations showing a time lag between phytoplankton blooms and bacterial increase (Ducklow, 1999); it is caused by the mixed DOM sources during the initial phase (passive leakage and heterotrophic sources) and the presence of allochthonous DOM. Algal-bacterial interactions during the intermediate phase resembled a microbial food web sensu Legendre & Rassoulzadegan (1995) with limited nitrogen uptake by the algae due to low DIN concentrations and limited ammonium regeneration by the bacteria. Bacteria were mainly depending on algal exudates and there was a direct transfer of ^{13}C from algae to bacteria such that the bacterial pool became fully labeled by day 6. During the stationary phase there was no regeneration of ammonia by bacteria and both algal and bacterial growth was nitrogen limited. This last stage resembles a typical microbial loop dominated ecosystem. There is some DOC accumulation during this stage, which is due to the 'malfunctioning of the microbial loop' caused by nutrient limitation of bacterial growth (Thingstad & Havskum, 1999), such that DOC uptake cannot keep pace with its exudation by phytoplankton.

The three phases have distinct ratios between bacterial and algal parameters. Bac-

terial to Primary production (BP:PP) ratios increased from 0.01 via 0.02 to 0.22 during the experiment. Similarly, bacterial carbon demand to primary production (BCD:PP) ratios increased from 0.06 at the beginning over 0.12 during the intermediate stage to 1.16 at the end. These ratios are often used to assess the metabolic status and functioning of ecosystems and to quantify coupling of phytoplankton and heterotrophic bacteria (Anderson & Ducklow, 2001; Morán *et al.* , 2002). High BCD:PP ratios indicate that bacteria dominate carbon flows and values higher than 1 imply an excess of carbon consumption by bacteria over algal production. This is often used as a measure of net heterotrophy, but care should be taken because BP and thus BCD are not constrained by PP (Jahnke & Craven, 1995; Strayer, 1988) and because changes in organic carbon stocks may support imbalances in production and consumption processes for some time (Fig. 5.2, 5.3).

5.4.4 Combined modeling and stable isotope approach

The coupled experimental-modeling approach we used provides unique opportunities to test and fine-tune our current state of knowledge of ecosystem functioning and more specifically of carbon and nitrogen coupling. Moreover, by the model we were able to analyze all the flows, even though only few of them have been measured. Models, as simple and crude as they may appear, capture our understanding of a system in mathematical terms and the consequences of this understanding, model output, is easily compared to observations. Our enclosure experiments were especially designed to allow model-data comparison. To describe the experiments, we chose a model complexity that was paralleled by the available data. This included combining a simple description of algal unbalanced growth that describes algae in terms of C and N (Tett, 1998) with a more complex bacterial growth model (Anderson & Williams, 1998), including two distinct DOC and DON pools with different biological lability. Although the experimental bloom evolved within a few days from a carbon and nitrogen balanced herbivorous/multivorous ecosystem to microbial loop system (Legendre & Rassoulzadegan, 1995), our simple model reproduced these changes in ecosystem functioning quite well and therefore provides an avenue towards generic ecosystem models.

The ^{13}C measurements, and especially the resolution of algal and bacterial compartments using specific PLFA biomarkers (Boschker & Middelburg, 2002), proved to be crucial to determine the phytoplankton exudation rates and the bacterial turnover rates. We had to find a delicate balance between reconciling the observed delay in bacterial ^{13}C uptake and reproducing the increased concentration of bacteria in the post bloom phase. Sensitivity analysis of the parameters (not shown) demonstrated that the initial slow bacterial uptake of ^{13}C was significantly influenced by the phytoplankton leakage rate. Moreover, the additional

DOC exudation by phytoplankton under nutrient limiting conditions influenced the bacterial ^{13}C content. Without the ^{13}C labeling, it would not have been possible to determine the DOC production and uptake rates; in that case it would not have been possible to distinguish exudated DOC from recycled DOC that comes from bacteria or detritus.

5.5 Appendix

Model parameters, variables, and model equations

Table 1: Model parameters

Symbol	Value	Units	Description	Source
α	0.015	μmol m^{-2} s^{-1} d^{-1}	Initial slope of P-I curve	A&W (recalculated)
ks_{DIC}	250	mmol C m^{-3}	Half-saturation ct for algal C uptake	Fitted
k_{Nn}	0.5	mmol N m^{-3}	Half-saturation ct for algal nitrate uptake	A&W
ks_A	0.5	mmol N m^{-3}	Half-saturation ct for algal ammonium uptake	A&W
Ψ	1.5	m^3 mmol N^{-1}	NH_3 inhibition ct for phytoplankton nitrate uptake	A&W
m_P	0.045	d^{-1}	Phytoplankton specific mortality rate	A&W
γ_1	0.02	-	Phytoplankton leakage fraction	Fitted
$r_{P,A}$	0.1	-	Phytoplankton activity respiration fraction	Assumed
$r_{P,B}$	0.01	d^{-1}	Phytoplankton basal respiration rate	Assumed
E	0.34	-	Phytoplankton mortality losses to DOM	A&W
γ_3	0.05	-	Ratio of extra DOC produced due to N limitation	Fitted
μ_P	5.5	d^{-1}	Phytoplankton maximum C uptake rate	Fitted
$\mu_{P,A}$	2	mol N mol C^{-1} d^{-1}	Phytoplankton maximum ammonium uptake rate	Fitted
$\mu_{P,Nn}$	2	mol N mol C^{-1} d^{-1}	Phytoplankton maximum nitrate uptake rate	Fitted
$max\theta_P$	20	mol C mol N^{-1}	Maximum phytoplankton CN ratio	Soetaert et al. (2001)
$min\theta_P$	6	mol C mol N^{-1}	Minimum phytoplankton CN ratio	Soetaert et al. (2001)
$max\eta_P$	2	g Chl mol N^{-1}	Maximum Chlorophyll *a* to N ratio in phytoplankton	Soetaert et al. (2001)
$min\eta_P$	1.4	g Chl mol N^{-1}	Minimum Chlorophyll *a* to N ratio in phytoplankton	Soetaert et al. (2001)
θ_Z	6.625	mol C mol N^{-1}	Zooplankton CN ratio	Assumed (Redfield)
g	1.0	d^{-1}	Zooplankton maximal grazing rate	A&W
B	0.75	-	Zooplankton assimilation efficiency	A&W
p_1	0.333	-	Zooplankton preference for phytoplankton food	A&W
p_2	0.333	-	Zooplankton preference for bacterial food	A&W
p_3	0.333	-	Zooplankton preference for detrital food	A&W
k_g	1.0	mmol N m^{-3}	Half-saturation food concentration for zooplankton grazing	A&W
Φ	0.23	-	Feeding losses to DOM	A&W
$f_{Z,B}$	0.03	d^{-1}	Zooplankton basal respiration rate	Assumed
$f_{Z,A}$	0.25	-	Fraction of zooplankton C uptake that is respired	Assumed
m_Z	0.3	d^{-1}	Zooplankton specific mortality rate	A&W
K_{mz}	0.2	mmol N m^{-3}	Zooplankton half-saturation for mortality	A&W
μ_B	13.3	d^{-1}	Maximum bacterial labile DOC uptake	A&W
μ_S	4	d^{-1}	Maximum bacterial semilabile DOC hydrolysis rate	A&W
Ω	0.19	mol C mol C^{-1}	Bacterial gross growth efficiency	Fitted
θ_B	5.1	mol C mol N^{-1}	Bacterial CN ratio	A&W
k_L	25	mmol C m^{-3}	Half-saturation value for bacterial labile DOC uptake	A&W
k_A	0.5	mmol N m^{-3}	Half-saturation value for bacterial ammonium uptake	A&W
k_S	417	mmol C m^{-3}	Half-saturation value for bacterial semilabile DOC hydrolysis	A&W
m_B	0.05	d^{-1}	Bacteria specific mortality rate	Fitted
$\theta_{D,max}$	15	mol C mol N^{-1}	Maximal CN ratio of detritus	Assumed
$R_{C,max}$	0.29	d^{-1}	Maximal degradation rate of detrital C at 20°C	Assumed
$R_{N,max}$	0.33	d^{-1}	Maximal degradation rate of detrital N at 20°C	Assumed
Y	0.03	d^{-1}	Nitrification rate	A&W
Δ	0.65	-	Part of grazing and mortality DOM flux to labile DOM	Fitted
Q_{10}	2.0	-	Q_{10} for temperature dependent rates	Soetaert e.a. (2001)
Salinity	0.2			Measured
K	0.06	mmol C m^{-3} μatm^{-1} d^{-1}	Gas exchange coefficient	Fitted
PCO2atm	360	μatm	Partial pressure of CO_2 in the atmosphere	
KC1	4.3×10^{-7}	-	Dissociation ct of H_2CO_3 at 0. salinity and 20°C	
KC2	5.61×10^{-11}	-	Dissociation ct of HCO_3^- at 0. salinity and 20°C	
K0	3.7×10^{-2}	mmol C m^{-3} μatm^{-1}	Solubility of CO_2 in water (Henry's law), 0.2 salinity and 20°C	Millero (1995)

Table 2: Model variables and forcings

Variable	Unit	Description
State variables		
N_P	mmol N m^{-3}	Phytoplankton N concentration
N_Z	mmol N m^{-3}	Zooplankton N concentration
N_B	mmol N m^{-3}	Bacterial N concentration
N_D	mmol N m^{-3}	Detritus N concentration
C_P	mmol C m^{-3}	Phytoplankton C concentration
C_D	mmol C m^{-3}	Detritus C concentration
L_C	mmol C m^{-3}	Dissolved labile organic carbon
S_C	mmol C m^{-3}	Dissolved semilabile organic carbon
DIC	mmol C m^{-3}	Dissolved inorganic carbon (bicarbonate, carbonate and CO_2)
L_N	mmol N m^{-3}	Dissolved labile organic nitrogen
S_N	mmol N m^{-3}	Dissolved semilabile organic nitrogen
N_n	mmol N m^{-3}	Nitrate and nitrite concentration
A	mmol N m^{-3}	Ammonium concentration
$^{13}C_P$	mmol C m^{-3}	Phytoplankton ^{13}C concentration
$^{13}C_Z$	mmol C m^{-3}	Zooplankton ^{13}C concentration
$^{13}C_B$	mmol C m^{-3}	Bacterial ^{13}C concentration
$^{13}C_D$	mmol C m^{-3}	Detritus ^{13}C concentration
^{13}CLabDOC	mmol C m^{-3}	Dissolved labile organic ^{13}C
^{13}C SemiLabDOC	mmol C m^{-3}	Dissolved semilabile organic ^{13}C
^{13}C DIC	mmol C m^{-3}	Dissolved inorganic ^{13}C
Other variables		
F	-	Limitation factor of photosynthesis due to PAR
Q_C(DIC)	-	Limitation factor of photosynthesis due to DIC
$Q_{Nn}(N_n,A)$	-	Limitation factor of nitrate uptake due to nitrate and ammonium
Q_A(A)	-	Limitation factor of ammonium uptake due to ammonium
$UptN_P$	mmol N m^{-3} d^{-1}	Phytoplankton growth
M_P	mmol N m^{-3} d^{-1}	Phytoplankton mortality
$R_{P,B}$	mmol C m^{-3} d^{-1}	Phytoplankton basal respiration
$R_{P,A}$	mmol C m^{-3} d^{-1}	Phytoplankton activity respiration
E	mmol C m^{-3} d^{-1}	Extra DOC produced by phytoplankton due to N-stress
$UptC_P$	mmol C m^{-3} d^{-1}	Phytoplankton carbon uptake rate
$UptN_{n,P}$	mmol N m^{-3} d^{-1}	Phytoplankton nitrate uptake rate
$UptA_P$	mmol N m^{-3} d^{-1}	Phytoplankton ammonium uptake rate
θ_P	mol C mol N^{-1}	Phytoplankton C/N ratio
C_Z	mmol C m^{-3}	Zooplankton C concentration
G_P	mmol N m^{-3} d^{-1}	Zooplankton grazing rate on phytoplankton
G_B	mmol N m^{-3} d^{-1}	Zooplankton grazing rate on bacteria
G_D	mmol N m^{-3} d^{-1}	Zooplankton grazing rate on detritus
E_Z	mmol N m^{-3} d^{-1}	Zooplankton excretion rate
M_Z	mmol N m^{-3} d^{-1}	Zooplankton mortality rate

Table 2 continued

$AssC_Z$	mmol C m^{-3} d^{-1}	Carbon assimilation by zooplankton
$R_{Z,A}$	mmol C m^{-3} d^{-1}	Activity respiration of zooplankton
$R_{Z,B}$	mmol C m^{-3} d^{-1}	Basal respiration of zooplankton
R_Z	mmol C m^{-3} d^{-1}	Respiration of zooplankton
$AssN_Z$	mmol N m^{-3} d^{-1}	Nitrogen assimilation by zooplankton
C_B	mmol C m^{-3}	Bacterial C concentration
F_B	mmol N m^{-3} d^{-1}	Bacterial growth rate
R_B	mmol C m^{-3} d^{-1}	Bacterial respiration
$uptC_B$	mmol C m^{-3} d^{-1}	Bacterial uptake of labile DOC
$uptN_B$	mmol N m^{-3} d^{-1}	Bacterial uptake of labile DON
$uptA_B^*$	mmol N m^{-3} d^{-1}	Potential bacterial uptake of ammonium
BactDOChydrolysis	mmol C m^{-3} d^{-1}	Bacterial hydrolysis of semilabile DOC
M_B	mmol N m^{-3} d^{-1}	Bacterial mortality
E_B	mmol N m^{-3} d^{-1}	Net ammonium excretion of bacteria
υ	mmol N m^{-3} d^{-1}	Ammonium oxidation rate
DissolutionC	mmol C m^{-3} d^{-1}	Dissolution rate of detrital carbon
DissolutionN	mmol N m^{-3} d^{-1}	Dissolution rate of detrital nitrogen
θ_D	mol C mol N^{-1}	C/N ratio in detritus
η_P	g Chl mol N^{-1}	Chlorophyll to N ratio in phytoplankton
Chla	mg m^{-3}	Chla concentration, calculated from phytoplankton concentration
CO_2flux	mmol C m^{-3} d^{-1}	CO2-flux from water to air
$pCO_{2(}$water)	μatm	Partial pressure of CO2 in the water

Forcing functions		
I	μmol m^{-2} s^{-1}	Photosynthetically active radiation (PAR, hourly values)
pH	-	(Daily measurements)
T	°C	Temperature (daily measurements)

Table 3: Model equations:

(1) $$f(T) = e^{\ln(Q10)\frac{T-20}{10}}$$

Phytoplankton:

(2) $$\frac{dP_N}{dt} = (1-\gamma_1)uptN_P - G_p - M_P$$

(3) $$\frac{dP_C}{dt} = (1-\gamma_1)uptC_P - G_p\theta_P - M_P\theta_P - R_P$$

(4) $$uptN_P = uptA_P + uptN_{n,P} = (Q_{N_N}(N_n, A)\mu_{p,N_n} + Q_A(A)\mu_{p,A})(1-\frac{\min\theta_P}{\theta_P})P_C f(T)$$

(5) $$Q_{N_n}(N_n, A) = \frac{N_n \exp(-\psi A)}{k_{N_n} + N_n}$$

(6) $$Q_A(A) = \frac{A}{k_A + A}$$

(7) $$uptC_P = FQ_C(DIC)(1-\frac{\theta_P}{\max\theta_P})\mu_p P_C f(T)$$

(8) $$F = (1-\exp(-\alpha I/\mu_p)$$

(9) $$Q_C(DIC) = \frac{DIC}{ks_{DIC} + DIC}$$

(10) $$E = \gamma_3 FQ_C(DIC)(\frac{\theta_P - \min\theta_P}{\max\theta_P})\mu_p P_C f(T)$$

(11) $$R_{P,B} = r_{P,B}P_N f(T)$$

(12)

(13) $$R_{P,A} = r_{P,A}uptC_P$$

$$R_P = R_{P,B} + R_{P,A}$$

(14) $$M_P = m_p P_N f(T)$$

(15) $$M_P\theta_P = m_p P_C f(T)$$

Zooplankton:

(16) $$\frac{dZ_N}{dt} = AssN_Z - M_Z - E_Z$$

(17) $$AssN_Z = (1-\varphi)\beta(G_P + G_B + G_D)$$

(18) $$AssC_Z = (1-\varphi)\beta(G_P\theta_P + G_B\theta_B + G_D\theta_D)$$

(19) $$G_P = \frac{gZp_1P_N{}^2}{k_g(p_1P_N + p_2B_N + p_3D_N) + p_1P_N{}^2 + p_2B_N{}^2 + p_3D_N{}^2} f(T)$$

Table 3 continued

(20) $R_{Z,A} = AssC_Z \times f_{Z,A}$

(21) $R_{Z,B} = N_Z \times f_{Z,B} f(T)$

(22) $R_Z = R_{Z,A} + R_{Z,B}$

(23) $E_Z = AssN_Z - (AssC_Z - R_Z)/\theta_Z$

(24) $E_Z \leq 0$

$\Rightarrow$

$R_Z = AssC_Z - AssN_Z \times \theta_Z$

$E_Z = 0$

(25) $M_Z = \dfrac{m_z Z_N^{\,2}}{K_{\mu_z} + Z_N} f(T)$

Bacteria:

(26) $\dfrac{dB_N}{dt} = F_B - G_B - M_B$

(27) $uptC_B = \dfrac{\mu_B \theta_B B_N L_C}{k_L + L_C}$

(28) $uptN_B = uptC_B \dfrac{L_N}{L_C}$

(29) $uptA_B^* = \dfrac{\mu_B B_N A}{k_A + A}$

if $-E_B \leq uptA_B^*$:

(30) $F_B = uptC_B\, \omega/\theta_B$

(31) $R_B = uptC_B(1-\omega)$

(32) $E_B = uptN_B - U_C\, \omega/\theta_B$

if $uptN_B + uptA_B^* \leq uptC_B \times \omega/\theta_B$:

(33) $F_B = uptN_B + uptA_B$

(34) $R_B = F_B \theta_B (1/\omega - \omega)$

(35) $E_B = -uptA_B$

(36) $M_B = m_B B_N^{\,2} f(T)$

Detritus:

(37) $\dfrac{dD_N}{dt} = (1-\varphi)(1-\beta)(G_P + G_B + G_D) + (1-\varepsilon)M_P - G_D - DissolutionN$

Table 3 continued

(38) $$DissolutionC = R_{C,\max}(1-{\theta_D}/{\theta_{D,\max}})D_C f(T)$$

(39)

(40) $$DissolutionN = R_{N,\max}(1-{\theta_D}/{\theta_{D,\max}})D_N f(T) \quad \text{if } \theta_D \geq \theta_{D,\max}$$

$$R_{C,\max} < R_{N,\max}$$

(41) $$DissolutionC = 0$$

(42) $$DissolutionN = 0 \quad \text{if } \theta_D < \theta_{D,\max}$$

DOM:

(43) $$\frac{dL_C}{dt} = \gamma_1(E + uptC_P) + \delta\begin{bmatrix}(1-\gamma_1)E + \varphi(G_P\theta_P + G_B\theta_B + G_D\theta_D)\\ + \varepsilon m_P P_C + M_B\theta_B + DissolutionC\end{bmatrix}$$
$$+ BacterialDOChydrolysis - uptC_B$$

(44) $$\frac{dS_C}{dt} = (1-\delta)\begin{bmatrix}(1-\gamma_1)E + \varphi(G_P\theta_P + G_B\theta_B + G_D\theta_D)\\ + \varepsilon m_P P_C + M_B\theta_B + DissolutionC\end{bmatrix}$$
$$- BacterialDOChydrolysis$$

(45) $$\frac{dL_N}{dt} = \gamma_1 uptN_P + \delta\begin{bmatrix}\varphi(G_P + G_B + G_D)\\ + \varepsilon m_P P_N + M_B + DissolutionN\end{bmatrix}$$
$$+ BacterialDONhydrolysis - uptN_B$$

(46) $$\frac{dS_N}{dt} = (1-\delta)\begin{bmatrix}\varphi(G_P + G_B + G_D)\\ + \varepsilon m_P P_N + M_B + DissolutionN\end{bmatrix}$$
$$- BacterialDONhydrolysis$$

(47) $$BacterialDOChydrolysis = \mu_S \times B_N \times \frac{S_C}{k_S + S_C} f(T)$$

(48) $$BacterialDONhydrolysis = \mu_S \times B_N \times \frac{S_N}{k_S + S_C} f(T)$$

DIN:

(49) $$\frac{dA}{dt} = E_B + E_Z - vAf(T) - uptA_P$$

(50) $$\frac{dN_n}{dt} = vAf(T) - uptN_{n,P}$$

DIC:

(51) $$\frac{dDIC}{dt} = R_P + R_Z + R_B - uptC_P - E - CO_2 flux$$

Table 3 continued

(52) $CO_2\,flux = K \times (pCO_{2(water)} - pCO_{2(atm)})$

$pCO_{2(water)} = CO_2 / K_0$

$$CO_2 = DIC - [CO_3^{--}] - [HCO_3^-] = DIC \cdot \frac{H^+ \cdot H^+}{H^+ \cdot H^+ + K_{C1} \cdot H^+ + K_{C1} \cdot K_{C2}}$$

$H^+ = 10^{-pH}$

Chlorophyll *a*:

(53)

$$\eta_P = \min \eta_P + (\max \eta_P - \min \eta_P) \times \frac{\min \theta_P}{\theta_P} \times \frac{\max \theta_P - \theta_P}{\max \theta_P - \min \theta_P}$$

(54)

$Chla = \eta_P \times N_P$